JOURNAL OF GEOPHYSICAL RESEARCH, VOL. 102, NO. D21, PAGES 25,281-25,292, NOVEMBER 20, 1997

Atmospheric nuclei and related aerosol fields over the Atlantic: Clean subsiding air and continental pollution during ASTEX

A.D. Clarke, T. Uehara, and J. N. Porter

School of Ocean and Earth Science and Technology, University of Hawaii, Honolulu

Abstract. Meteorological conditions in the Atlantic Stratocumulus Transition Experiment (ASTEX) region favored advection of clean air from the central Atlantic during the early part of the experiment that was replaced by polluted air of European origin during the latter part of the experiment. Marked differences in the aerosol size distribution, composition, and state of mixing existed in these air masses. Pronounced differences in their vertical structure also demonstrated that surface measurements often do not represent average boundary layer or column concentrations. Clean subsiding air from the free troposphere had concentrations of condensation nuclei that significantly exceeded concentrations in the boundary layer and had very low mass concentrations and volatility consistent with homogeneous nucleation aloft, supporting the hypothesis that these nuclei can provide a source for "new" nuclei into the marine surface layer. This finding was in contrast to polluted air characterized by high concentrations of aged aerosol but having no evidence for significant recent nuclei formation. Particles in polluted air consisted of more than 90% volatile mass (mostly sulfate) and a refractory residual remaining at 300°C. The refractory mass varied with the concurrently measured light absorption coefficient, associated with combustion-derived soot. In spite of 2 orders of magnitude more volatile sulfate in polluted air, most of the particle number in polluted air remained after volatilization at 300°C, in contrast to less than 10% in clean air. This finding suggests that the number of particles in polluted air may reflect the combustion process producing the primary soot aerosol more than the SO_2 emissions responsible for much of the sulfate aerosol mass. The accumulation mode mass mean diameter was found to increase with total accumulation mode mass, suggesting that a size parameterization based upon the more commonly measured sulfate mass could be included in current aerosol models.

1. Introduction

During June1992 we participated in the Atlantic Stratocumulus Transition Experiment (ASTEX) program aboard the National Center for Atmospheric Research (NCAR) Electra as part of the Marine Aerosol and Gas Exchange (MAGE) program. Flight missions [*Huebert et al.*, 1996] focused upon aerosol and gas phase measurements in conjunction with other platforms studying issues related to the development and evolution of stratus clouds in the Azores region. Our specific objectives included radiative closure in the lower troposphere [*Clarke et al.*, 1996a], aerosol evolution during Lagrangian advection in the marine boundary layer (MBL) [*Clarke et al.*, 1996b], and a characterization of the microphysics and chemistry of aerosol types present in the North Atlantic (this paper).

The last objective is related to the need for appropriate models of aerosol physicochemistry, particularly for characterizing remote marine aerosol [*Penner et al.*, 1993]. Model inputs require vertically resolved information on size dependent properties related to radiative effects [*d'Almeida et al.*, 1991] and properties affecting their ability to act as cloud condensation nuclei (CCN). For example, a given aerosol mass concentration may have very different optical properties depending upon the effective mass mean diameter and composition [*Bergstrom*, 1973]. Refined parameterizations are also needed for fundamental properties of remote marine aerosol and the processes that govern their evolution under both clean and continentally influenced conditions [*Benkovitz et al.*, 1994]. These include the nature of the nucleation process in remote regions, aerosol evolution during transport, aerosol gradients, and the representativeness of existing surface-based measurements for assessing column properties or validation of model predictions.

Paper number 97JD01555.
0148-0227/97/97JD-01555$09.00

2. Instrumentation

The aerosol measurements and their interpretation discussed in this paper are based upon the following instrumentation. All sample air aspirated into the aircraft through a sampling inlet that has been characterized for losses [*Porter et al.*, 1992] and measured at low relative humidity (RH<25%). Continuous measurements and relevant flight information were logged and saved as 15 s averages.

1. Laser optical particle counter (OPC) (Particle Measurement Systems LAS-X, Boulder, Colorado; modified for 256-channel resolution) yields particle size distributions nominally from 0.14 to 7.0 μm diameter. Aerosol is preheated to 40°C, 150°C, and 300°C to infer aerosol composition from volatility [*Clarke*, 1991].

2. Condensation nuclei (CN) counter (Thermal Systems Inc. 3760) counts total particle number from 0.015 to 3.0 μm. A second unit operated at 300°C counts "refractory CN" (RCN) remaining at 300°C.

3. Ultrafine condensation nucleus counter (UCN) (Thermal Systems Inc. 3025) counts particles between 0.003 and 3.0 μm. The difference between UCN and CN counter indicates recently formed particles present in 0.003 and 0.015 μm range.

4. Scanning differential mobility analyzer (DMA) (Thermal Systems Inc. 3071) sizes particles into 17 size bins 0.02 and 0.55 μm with thermal analysis similar to the OPC. Arcing problems and other difficulties resulted in fewer data than we desired, particularly at smaller sizes.

5. Aethaelometer (Magee Scientific - AE9) an optical measurement of light attenuation by particles on a filter yielding an estimate of the concentration of black carbon (BC) and the related aerosol light absorption coefficients. See appendix for sampling concerns.

This instrumentation provided real time assessment of physical, chemical, and optical properties of the aerosol. Differences between aerosol types were generally revealed by variations in the aerosol size distribution. The DMA characterized those sizes that dominated the number concentration of CN in the atmosphere, while the OPC characterized sizes that include most aerosol mass. Both instruments employed thermal volatilization to infer the composition and state of mixing of the aerosol, properties related to their formation and evolution. The term "refractory" here refers to aerosol remaining after heating to 300°C, a temperature that volatilizes acrosol sulfuric acid and ammonium sulfate (and some other species including some organic species). Most refractory aerosol mass is essentially dust, sea salt, or soot, all of which originate primarily at Earth surface.

3. Results

This rapid characterization of aerosol physicochemistry revealed the detailed three-dimensional structure present and the complexity of aerosol fields in the ASTEX region. These aerosol fields included clean air subsiding from above the central Atlantic, pollution advected from Europe, desert dusts transported from the Sahara and marine aerosol produced in the marine boundary layer (MBL). Because changes in the size distribution, concentration, and volatility of these particles can reflect these characteristics and their dynamic evolution in the atmosphere, we illustrate here a few examples that demonstrate these properties.

The mass of most aerosol species is generally concentrated in diameters (Dp) greater than about 0.1 μm that are best resolved in our system with our OPC data. Because dry volume (mass) is the most commonly described characteristic, we will introduce these distributions first for the common aerosol types that we encountered on ASTEX (Figure 1). In this linear/log format the

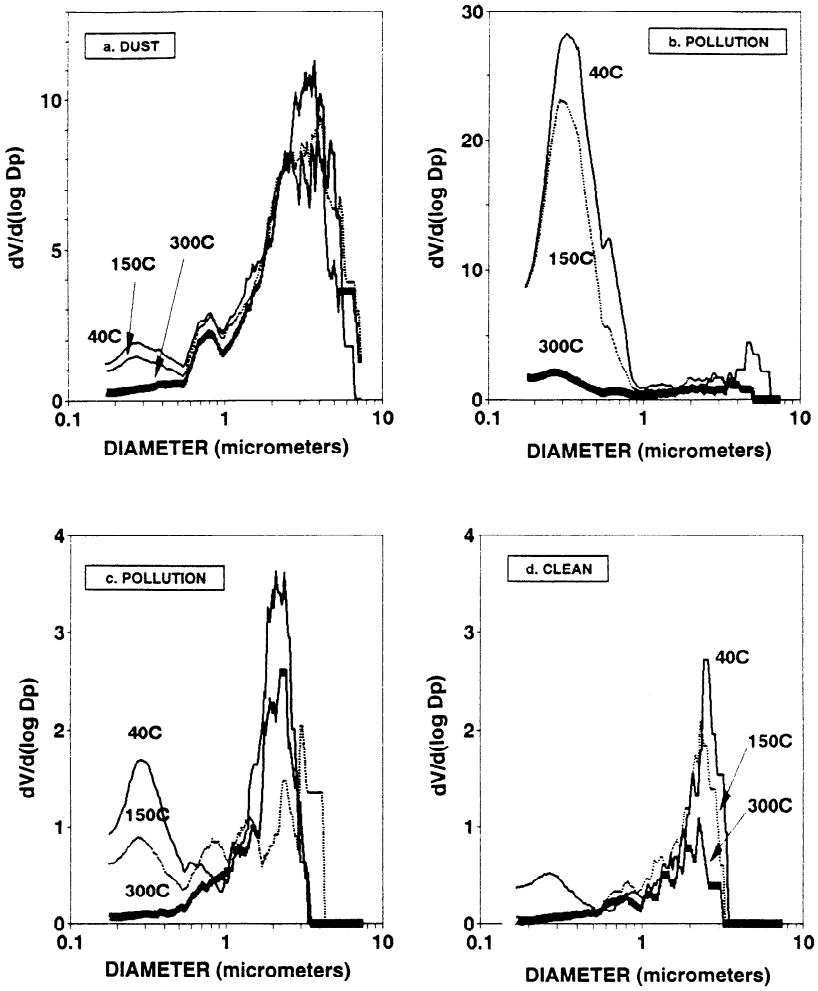

Figure 1. OPC volume size distributions ($\mu m^3 cm^{-3}$) for indicated dates and times at three temperatures in (a) dust plume aloft (2800 m, June 16, 1992, 1423), (b) concentrated pollution (1050 m, June 15, 1992, 1313), (c) dilute pollution near surface (440 m, June 15, 1992, 1503) and (d) clean air near surface (440 m, June 15, 1992, 1512).

area under the indicated distributions is proportional to aerosol volume. A rough estimate of the dry mass distributions can be obtained by simply multiplying the volume distribution scale by 1.8 (the density for ammonium sulfate 1.8 g cm^{-3}) to yield mass concentrations in μg m^{-3}. The greatest concentrations of coarse particles (Dp>1 μm) were found in dust cases, shown in Figure 1a. The sharp truncation of the distribution near the upper size limit reflects the loss of particles in the sampling inlet above about 4 μm [*Porter et al.*, 1992] and indicates that dust sizes probably extend to diameters larger than those shown here. The three sequential OPC thermal scans, also shown, indicate the presence of a volatile sulfate peak near 0.2-0.5 μm. The difference evident between 40°C and 150°C indicates the maximum sulfuric acid volume that might be associated with this aerosol, while the 150°C-300°C difference indicates the maximum neutralized sulfate that might be present [*Clarke*, 1991]. The refractory residual at 300°C is interpreted as the tail of the dust or sea-salt distribution (see discussion below).

Figure 1b is an example of a pollution plume case in which fine particle sulfate aerosol dominates the volume (mass). Volatility evident in Figure 1a suggests a nearly neutralized fine mode with a fine particle residual (refractory) remaining after heating to 300°C. Later we show that this residual is associated with a Black Carbon (BC) component. Figure 1c is case of near-surface pollution mixed with clean marine aerosol such that the fine sulfate peak is less than the apparent coarse sea-salt peak. (When we compare with Figure 1a, what appears as truncation at smaller diameters in Figures 1c and 1d for surface aerosol is actually due to the evaporation of these sea-salt aerosol (sampled "wet" at the inlet tip) to their dry diameters that occurs after the inlet loss but before measurement by the OPC). Increased volatility present in Figure 1c at 150°C is interpreted as a relative increase in the sulfuric acid component. A near-surface clean air case is shown in Figure 1d. The fine particle concentration is both the lowest of those shown and also completely volatile at 300°C, indicative of a fine particle sulfuric acid aerosol superimposed on the tail of a coarse sea-salt aerosol. All of the cases introduced in Figure 1 will be referred to in specific context later in the text. These differences inferred from the rapid response sizing using the thermal OPC demonstrates the advantage of this indirect approach for sampling from aircraft.

3.1 Clean Air Aerosol

The "clean air" aerosol cases encountered during ASTEX were typified by low sulfate and BC (soot) concentrations below 25 ng m^{-3}. Those trajectories were predominately from the central North Atlantic [*Huebert et al.*, 1996; *Jensen et al.*, 1996] and indicate a subsiding air mass [*Bretherton and Pincus*, 1995]. CN concentrations near the surface and exposed to below-cloud scavenging dropped as low as 25 cm^{-3} at times, and not unlike Antarctic values [*Bodhaine*, 1983], but more typical values were near 200-300 cm^{-3}. Concentrations in clean air aloft were often several thousand per cubic centimeter but were associated with low aerosol mass concentrations of about 0.1 μg m^{-3} (see below).

The DMA sizes particles over the part of the aerosol spectra that describes most of the CN population. DMA number and volume distributions at both 40°C and 300°C for this clean subsiding Atlantic air at 2800 m is shown in Figure 2. The majority of the accumulation mode volume (mass) peak at 0.2 μm (Figure 2a) is lost upon heating, leaving a refractory residual. Because BC concentrations were very low in this air (see below), this refractory component is interpreted as the lower "tail" of a residual sea-salt and/or dust distribution. The apparent minimum at 0.25 μm is a consequence of low count statistics for the larger particles, resulting in a perturbed DMA size inversion process, and should be ignored.

We have indicated that the number and volume (mass) distributions for this aerosol can be reasonably described by two superposed lognormal fits. To establish these, we made a lognormal fit to the measured "dry" accumulation mode mass distribution, step 1 in Figure 2a. Using the properties of lognormal distributions [*Seinfeld*, 1986], we can describe the lognormal number distribution associated with this mode as shown in Figure 2b. Next, the subtraction of the fitted accumulation mode number from the measured number distribution in Figure 2b results in a nuclei number distribution that can be approximated with a second lognormal, step 2 in Figure 2b. Because diffusive loss generally results in undercounting in the lowest DMA channels, a small adjustment in the smallest channel has been included. This fitted number distribution is then presented as the small particle volume distribution shown in Figure 2a. This overlapping bimodal lognormal nuclei number distribution is also in agreement with constraints imposed by the nuclei counters.

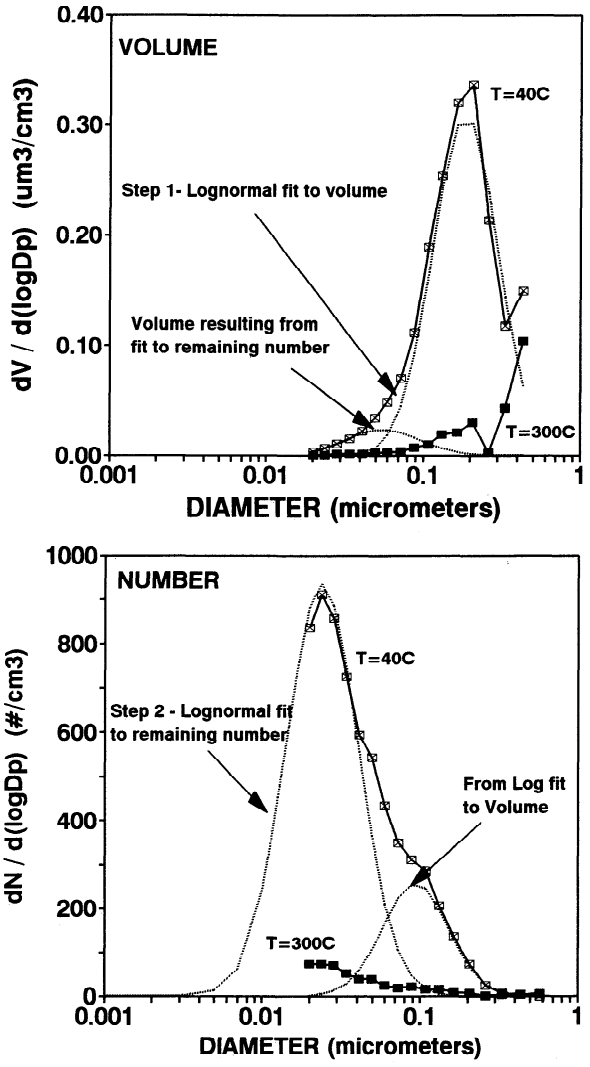

Figure 2. Measured DMA number and volume distributions (boxes) for flight 7 clean air case on June 14, 1994 at 2800 m. A lognormal fit to volume and number distributions are indicated (dotted lines) as described in text.

Together, Figures 2a and 2b show that about 90% of both mass and number were removed by heating. This finding indicates that most of the volatile mass in Figure 2a was associated with particles that are completely volatile, a behavior expected for particles formed in - situ by homogeneous nucleation. These data imply that for this air mass the refractory CN constitute only a small fraction of the total CN. In comparison with more polluted DMA distributions and even "clean" near-surface values (see below and *Jensen et al.* [1996]) the number peak near 0.02 μm is at small diameters indicative of recently nucleated aerosol. We surmise that the larger mass peak near 0.2 μm is the residual mass from air previously carried aloft, possibly through cloud pumping [*Chatfield and Crutzen*, 1984], in which nucleation subsequently occurred in accord with previous observations [*Clarke*, 1993a] and models [*Raes and VanDingenen*, 1992; *Raes*, 1995]. Although we describe the distribution as bimodal, the intermode minimum is less pronounced than that expected to result from cloud processing and growth of a broad distribution [*Hoppel et al.*, 1990]. This situation would be expected for aerosol formed aloft that has not passed through cloud.

3.2 Continental Pollution Aerosol

Size distributions were markedly different in continentally influenced air masses that were marked by high sulfate and BC concentrations that contributed to a visible haze extending up to several kilometers altitude. DMA volume and number distributions in this polluted air are shown in Figures 3a and 3b. The distribution in Figure 3a is about 40 times greater in total volume than in clean air (Figure 2a), and it is shifted to a mass mean diameter near 0.3 μm. This finding indicates that there are both more and larger nuclei in the polluted case than in the clean case. Upon heating to 300°C most of the pollution aerosol volume (mass) is lost, as was seen in the clean case, but the refractory volume now has a clear refractory mass peak at a diameter of about 0.17 μm. When presented as a number distribution in Figure 3b, the residual refractory distribution is about a factor of 5 smaller in diameter but with a number concentration only about 30% less than the original unheated sample. Our interpretation of this behavior is that much of the volatile fine particle mass (primarily sulfate) exists as "coatings" that accumulated upon a smaller refractory aerosol. Because the DMA distribution includes most of the total CN, these refractory CN (RCN at 300°C) constitute a large fraction of the total, in contrast to the small fraction of the CN that remain after heating in clean air shown in Figure 2b. This size- resolved volatility in the CN distribution constitutes a basis for continuous characterization of aerosol by the RCN/CN ratio, to be discussed below.

3.3 Continental Dust Aerosol

A third type of air mass was influenced by passage over North Africa and included high concentrations of coarse Saharan dust aerosol [*Prospero and Carlson*, 1981]. This was primarily encountered during the latter part of the ASTEX experiment and was concentrated above 2 km altitude and over the continental pollution aerosol found nearer the surface. The peak concentration was often near 4 km, but at intermediate altitudes between 2 and 2.5 km a mixed dust and pollutant aerosol was observed [*Clarke et al.*, 1996a]. Because dust dominates the coarse aerosol size range, these distributions are best characterized by the OPC. A representative distribution is shown in Figure 1a during the June 16 flight leg at 2.8 km. The coarse refractory dust component is evident at all temperatures. Note that the "peak"

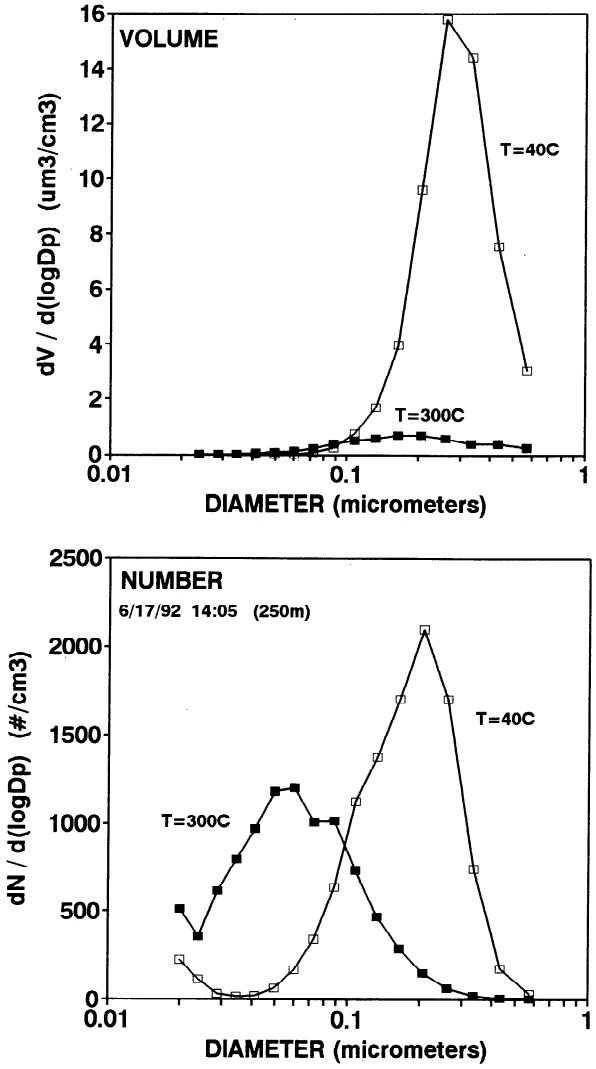

Figure 3. DMA number and volume distributions typical for polluted air during ASTEX (as in Figure 2).

near 0.7 μm is an artifact of the Mie scattering in the OPC instrument. Otherwise the "tail" of the refractory dust distribution steadily decreases at smaller sizes. For short sample times (about 3 min) the low number concentration of dust particles results in poor count statistics, and the differences evident in the heated scans simply indicate dust variability over the sample period [*Clarke et al.*, 1996b) rather than relative volatility.

The volume distribution in Figure 1a is clearly dominated by coarse particle dust at larger sizes, but the volatile component present at smaller sizes below 0.5 μm reveals the contribution of sulfate aerosol to this size class. The three temperatures used here also show little volatility at 150°C for the fine particle aerosol and suggest that no more than 20% of the fine particle mass could be present as sulfuric acid [*Clarke*, 1991]. This is an example of mixed dust/sulfate that occurred at altitudes between 2 and 3 km, apparently due to mixing of the nearly pure dust aerosol above with the pollution aerosol below [*Clarke et al.*, 1996a].

The strong horizontal gradients present in these dust "plumes" aloft are shown in Figure 4 data from flight 11 on June 19, 1992. A example leg flown at 3110 m is shown as an inset in Figure 4, and the regions that correspond to the illustrated size distributions are shown by a number. This flight was one of the "Lagrangian

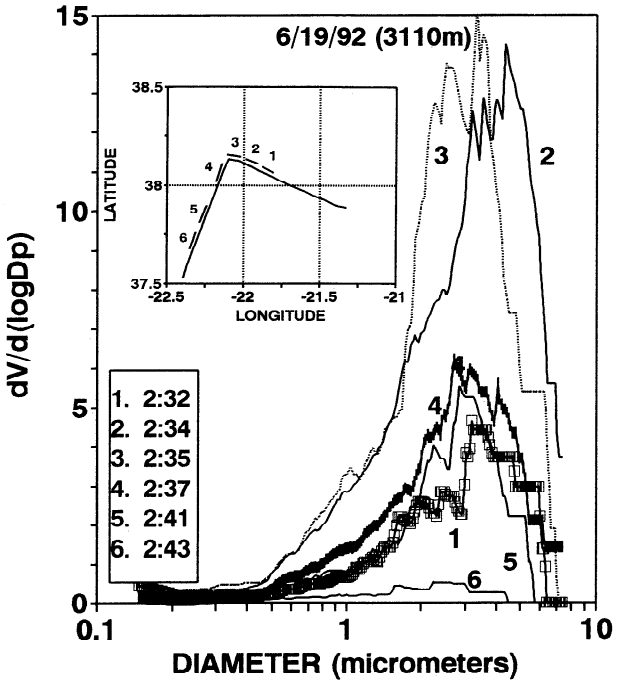

Figure 4. Six sequential OPC volume size distributions ($\mu m^3\ cm^{-3}$) collected June 19, 1992 along a 3110 m altitude flight leg illustrated in inset. Marked gradients are present on scales of about 15 km with high concentrations near the apex of the turn.

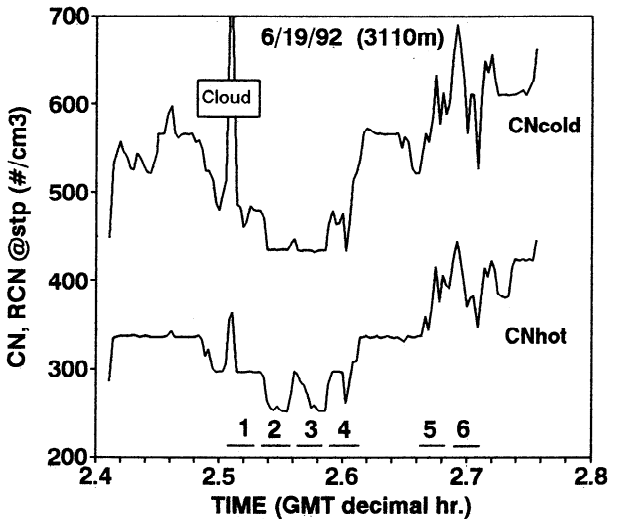

Figure 5. Plot of CN cold and CN hot for the same leg shown in Figure 4. Minimum concentrations occur in regions of maximum dust particle mass.

evolution" experiments [*Clarke et al.*, 1996b; *Huebert et al.*, 1996]. These missions consisted of L - shaped legs with crosswind and downwind legs that were flown at various altitudes and advected with the wind. On these flights we followed a European pollution aerosol below the inversion with varying aerosol aloft that moved with speeds and directions different from those in the mixed layer air. The largest values shown for dust volume in Figure 4 are within about 20% of those shown in Figure 1a, but negligible sulfate is associated with the dust at this altitude. These six near-sequential samples (one missed between 4 and 5 due to data disk change) represent variations in concentration of about a factor of 40 in coarse particle mass during the 9 min of flight and about 45 km track distance. Concentrations start out at intermediate values, reach a maximum just near the turn, and then decrease rapidly (3 to 4) as we head SW away from the turn. They then decrease more slowly (4 to 5) before dropping rapidly to very low values (5 to 6).

The associated CN counts along this track are shown in Figure 5. The opposite trend in CN counts is evident here with the lowest CN associated with regions of highest dust loading and higher counts in the "clean" air with lowest dust concentrations. This is the same observation we have reported elsewhere in the free troposphere over the Pacific [*Clarke*, 1993a] and on other more recent field studies (unpublished data). Hence, unlike behavior expected near pollution sources, in remote air masses the aerosol number tends to increase as aerosol mass decreases. More extensive discussion of vertical gradients in dust aerosol during ASTEX can be found elsewhere [*Clarke et al.*, 1996a, Figure 7] and will not be repeated here.

3.4 Adjacent Clean-Polluted Aerosol Fields: June 15, 1992

The differences in aerosol microphysical properties and chemistry evident in the size distributions illustrated above were characteristics of large-scale aerosol fields present during ASTEX. On June 15, 1992, we encountered clean and polluted adjacent air masses in the MBL with very different spatial structure and composition. Figure 6 shows the calculated back trajectories (C. Bretherton, University of Washington) from the vicinity of our measurement region (33°N, 25°W). A polluted air mass below the inversion is located to the east of a subsiding clean air mass from the central Atlantic described above. The back trajectories indicate that the polluted air mass passed over central Europe about 2 days earlier (C. Bretherton, personal correspondence 1996).

Some of the structure within these two distinct aerosol fields is revealed in Figure 7a. This shows a time series of aircraft altitude, BC, and ozone for the entire flight and includes an inset of the flight path showing the location of stacked flight legs carried out in both air masses. Because BC is a constituent of most

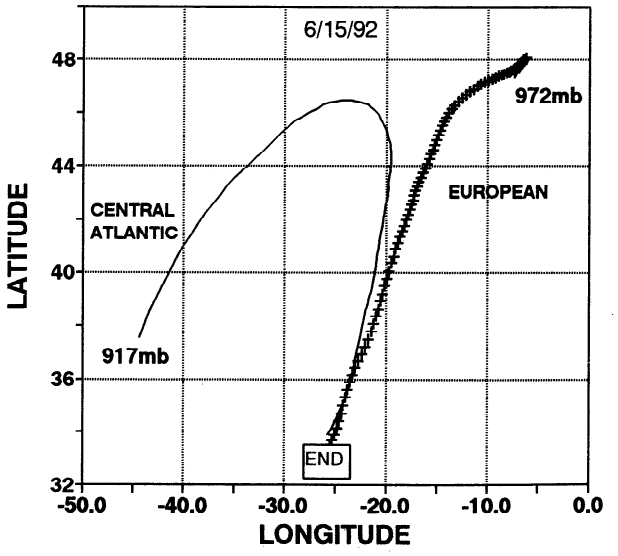

Figure 6. Trajectories for boundary layer adjacent clean central Atlantic (fine line) and polluted European (hatched line) air masses measured on June 15, 1994.

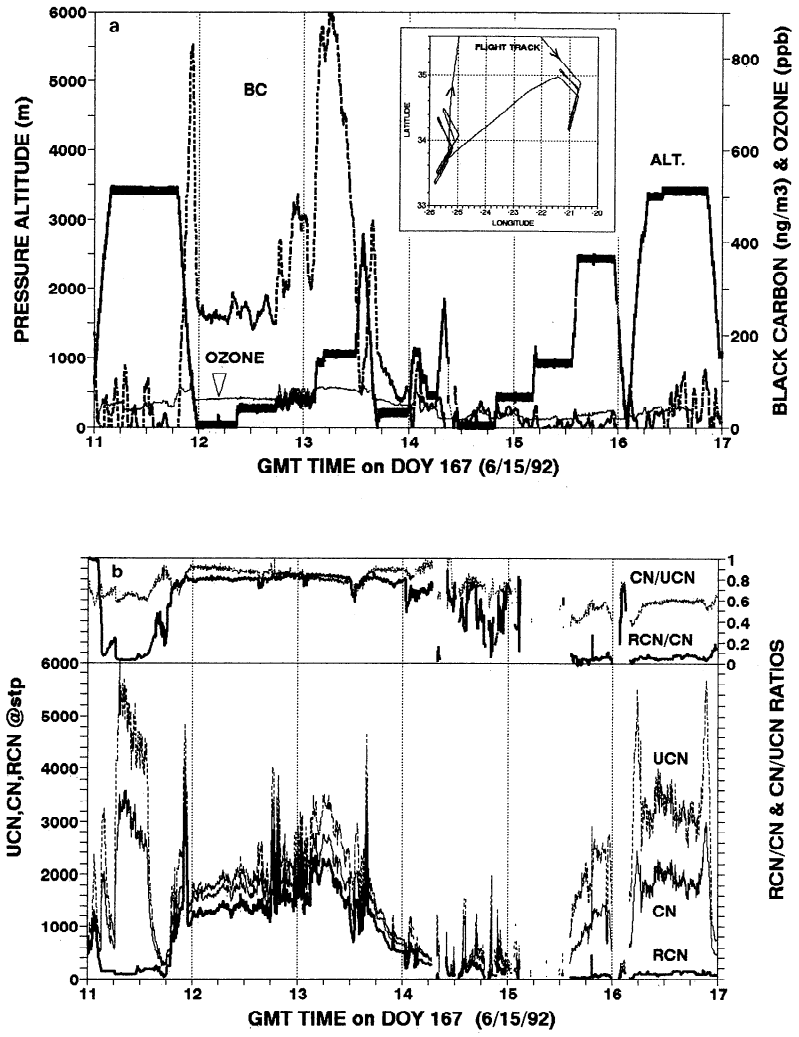

Figure 7. (a) Time series of altitude (—), black carbon (– – –), ozone (——) for June 15 flight. Inset shows flight legs, (b) Time series for CN, UCN, RCN (per cubic centimeter), with CN/UCN and RCN/CN as indicated in figure for June 15 flight.

combustion aerosol, it provides a clear pollution indicator. A careful look at the first descent (35°N, 21°W) reveals that the maximum BC occurs well above the surface, as confirmed in the maximum values observed for the horizontal stacked legs near 1000 m altitude at about 1315. A marked transition from polluted to clean air is also evident in BC concentration at about 1400 as the aircraft moves west near 34°N, 25°W. Ozone is also seen to vary in conjunction with BC in polluted regions but not in clean regions.

A typical OPC volume distribution (Figure 1b) reveals the aerosol volatility characteristic of the polluted region. The submicrometer accumulation mode (volume mean diameter at 0.32 μm) aerosol dominates the aerosol volume (mass), which totals about 25 μg m^{-3} (assumed dry density of 1.8 g cm^{-3}) and exceeds even the coarse dust concentrations shown in Figure 1a. The figure also reveals the small change in volume upon heating from 40°C to 150°C, indicative of little sulfuric acid being present. Much greater mass is lost upon heating to 300°C, but a significant residual component with diameters near 0.25 μm remains. Because our volatile fine particle mass inferred from the OPC agrees within about 20% of the total fine particle sulfate measured [*Zhuang and Huebert*, 1996], we interpret most of this volatile mass to be sulfate. However, some of this difference may reflect other species such as organic material. The temperature dependence shown in Figure1b suggests an ammonium to sulfate molar ratio of about 0.75 [*Clarke*, 1991]. The residual submicrometer peak (Dp<0.5 μm) at 300°C is only pronounced in the OPC data for the pollution aerosol and is related to the refractory BC component of the aerosol (see below). The larger (Dp > 0.5 μm) refractory aerosol in this distribution and others is interpreted as either sea salt or dust, depending upon conditions.

The transition region to cleaner air near 1400 UT (Figure 7a) was marked by clouds, drizzle, and at times significant rainfall. The spatial scale of this mixing and transition shows up in the apparent BC and ozone peaks during the flight legs near the surface and 400 m at 1435 and 1500, respectively. These peaks are centered about the "turn" region (near 34°N, 25°W) for each of these legs with a transition to even cleaner air near the northern ends. Figures 1c and 1d reveal the changes in two sequential OPC size distributions and their volatility collected about 9 min apart between the middle and end of the leg. The volatility continues to be consistent with a neutralized ammonium sulfate having a molar ratio near 0.6 [*Clarke*, 1991], although the concentrations in the pollution-influenced region near the turn are an order of

magnitude lower than the main plume shown in Figure 1b. By the end of this leg (Figure 1d) the refractory residual is further diminished, and the submicrometer peak is completely volatile by 150°C, except for the tail of the sea salt, suggesting a sulfuric acid composition. This variability in aerosol physicochemical properties reflects the narrow boundary between two air masses of large regional extent. This small-scale structure is generally obscured by longer-period averages required for typical techniques employed for aerosol chemistry.

Figure 7b shows the time series for the CN, RCN and UCN corresponding to the data in Figure 7a. The narrow spikes and periods of deleted data (e.g., 1515) in the nuclei data are a result of cloud droplet shatter on the inlet probe (see appendix). At other times the variability in nuclei evident in the polluted air (around 1145-1400) in Figure 7b tracks the variability in BC (Figure 7a), reflecting their common source. However, in clean air with low BC (e.g., 1530-1650), poor signal to noise for the differential BC measurement obscures any relationship.

Note that in spite of the fundamental differences in DMA data for both air masses shown above (Fiures.2 and 3) the concentration of CN in both air masses can be similar (Figure 7b; compare 1315 with 1630), while RCN are dramatically different. This fundamental difference is also expressed in the far more rapid and simple measurement of the RCN/CN ratio for these air masses (0.8 and 0.1, respectively) as shown at the top of Figure 7b. This ratio indicates the fraction of CN that are refractory or have a refractory component. In spite of the considerable variability in the nuclei concentrations this ratio stays steady at low (high) values in clean (polluted) air masses and exhibits changes in the transition region (1400-1500) that reveals the small-scale mixing of these air mass types.

A second ratio of the CN measured with the TSI3760 (Dp>20 nm) to the total UCN (Dp>3 nm) measured with the TSI3025 is also included in Figure 7b. Ratios near 1 indicate few nuclei are present in the 3-20 nm range but lower values indicate an increasing fraction of small nuclei in this size range. This ratio also shows little variation with short-term fluctuations in nuclei concentration but does show differences between air mass type as well as with altitude in the polluted region. Clean regions aloft (e.g., 1130 and 1630) have a greater fraction of these smaller nuclei. The clean air mass near the surface (1430-1500) also has lower values for the CN/UCN ratio than polluted near-surface air (1200-1230). These observations are consistent with the differences in the size distributions compared in Figures 2b and 3b. Also note that near 1135 a similar sharp transition region from clean to polluted air is also present aloft (3500 m) at about 10 min (60 km) prior to our first descent profile.

3.5 Vertical Profiles

Differences in the vertical structure of aerosol properties in the two regions are revealed in Figures 8a and 8b for BC, CN, RCN, and RH. For the pollution region (Figure 8a) it is clear that BC, CN, and RCN are closely related and all go through maximum values in a relatively dry layer between the top of the surface marine layer [*Martin et al.*, 1994] at about 350 m and the main inversion near 2000 m. Accumulation mode mass (not shown) in this region is of the order of 10 $\mu g\ m^{-3}$ with a maximum of about 25 $\mu g\ m^{-3}$ occurring at the peak CN concentration. A decreasing tendency in all nuclei and the RCN/CN ratio can be seen above the inversion. The surface values shown for BC (around 250 ng m^{-3}) and CN (around 1300 cm^{-3}) are less than one third of the concentrations in this concentrated layer aloft but agree well with surface shipboard data taken in the regions of elevated pollution [*Jensen et al.*, 1996]. In the moist well-mixed below-cloud surface marine layer, all aerosol components are substantially reduced in relation to the peak pollution layer. This reduction reflects the decoupling of this pollution layer from the well-mixed surface layer and suggests a gradual erosion of the base of the pollution layer by mixing, entrainment, and scavenging from below during advection over the ocean [*Martin et al.*, 1994].

A very different picture is evident from the profile in the clean air to the west (Figure 8b). BC concentrations are low and usually in the noise of the differential measurement from this instrument for the short averaging times needed for a descent profile. Unlike the pollution case, in this clean case the CN actually increase with altitude (Figure 8b) to values aloft that are higher than in the polluted air but with aerosol mass concentrations that are more than 2 orders of magnitude lower (about 0.1 $\mu g/m^3$). These CN concentrations are shown corrected to STP so that they are conserved with regard to pressure changes related to vertical motions. Concentrations aloft are also more than an order of magnitude greater than clean air near the surface in this figure and values measured over longer periods aboard ship [*Jensen et al.*, 1996]. The RCN concentrations are also low and decrease with increasing altitude. Both observations are consistent with a source of volatile aerosol from aloft and, in keeping with prior observations, indicate that these particles appear to be nucleated prior to subsidence [*Clarke*, 1992, 1993a]. Again, the spikes in the CN and RCN data are an artifact caused by the shatter of saline droplets on our inlet probe (see Appendix) both in cloud and in precipitation.

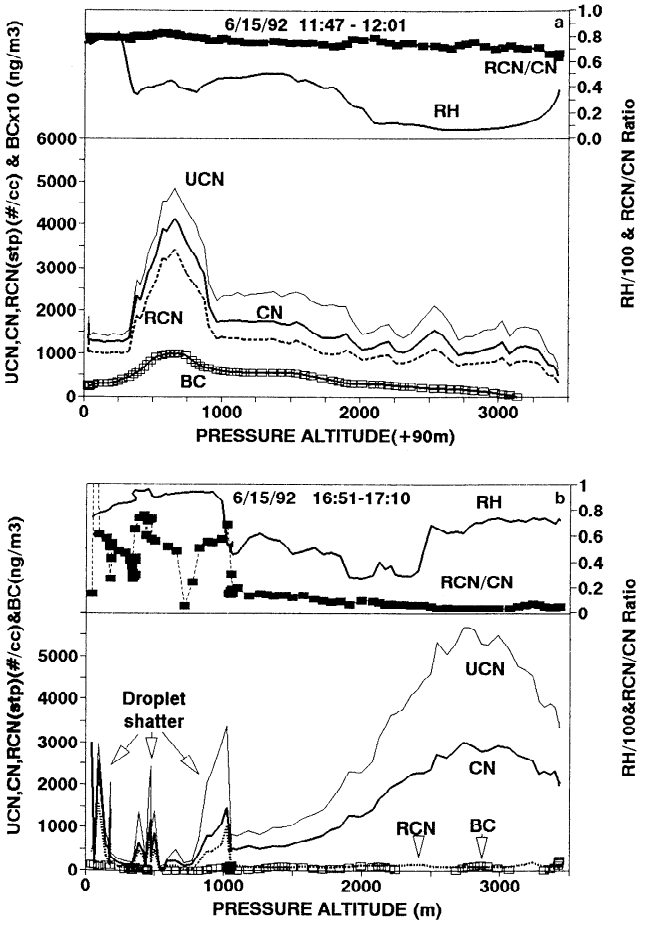

Figure 8. Vertical profiles contrasting (a) polluted and (b) clean (b) air shown in Figure 7.

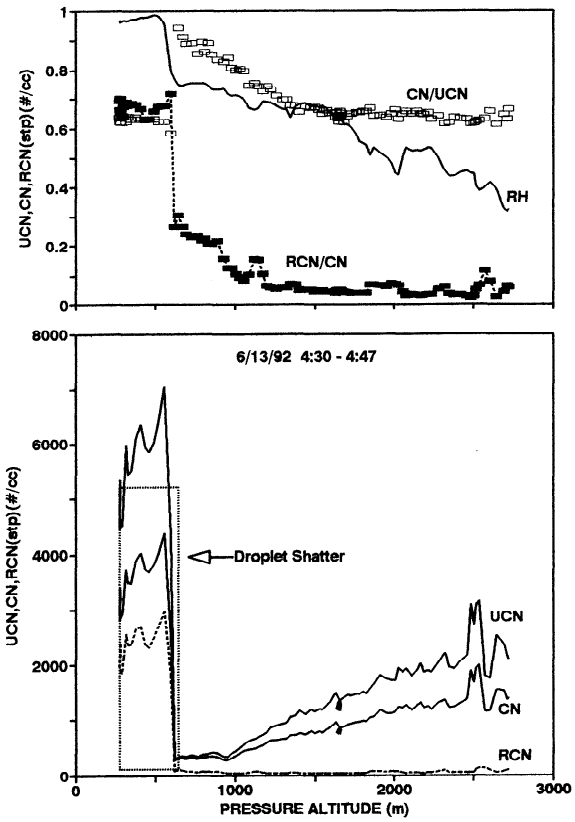

Figure 9. "Typical" vertical profile for clean air day.

The clean air descent profile shown in Figure 8b is the most pronounced example of higher nuclei concentrations aloft characteristic of several ASTEX clean air profiles. Flight 6 on June 13 is a more representative case with no clouds above 700 m (Figure 9). All profiles in this subsiding air [*Bretherton and Pincus*, 1995; *Huebert et al.*, 1996] showed a similar increase in CN with altitude. Unlike the polluted profiles (Fig. 8a) the BC concentrations both aloft and at the surface were in the noise of the measurement. OPC size distributions measured during this descent profile (Figure 10) have far lower concentrations at all altitudes than the cases shown in Figure 1a but reveal a significant increase on descent below 1200 m (Figure 10, number 4) at the same location at which the RCN/CN ratio starts increasing in Figure 9. Once again this mass increase during descent is accompanied by a decreasing number (Figure 9). Unlike most ASTEX flights the volatility observed in OPC data throughout the "clean" MBL is indicative of a sulfuric acid aerosol and similar to that illustrated in Figure 1d.

The above data for the ASTEX/MAGE study region provides examples of the aerosol types, gradients and variability for clean and polluted marine air masses over the western North Atlantic. Specific features of the data are summarized here:

1. In the polluted region, CN, RCN, and UCN all track with each other and with BC, reflecting a common source. In the clean region, CN and UCN track each other but are not clearly related to BC or RCN that are low.

2. In the polluted region, UCN, CN, and RCN concentrations agree within about 15% (Figure 7b), with few particles smaller than 20 nm, but in the clean region, about 40% of the UCN are smaller than 20 m diameter.

3. The small reduction in CN number upon heating to 300°C (Figure 3b) reveals that most pollution CN include a refractory component.

4. CN and UCN in clean subsiding air exceed STP concentrations in the boundary layer and reveal a gradient from aloft toward the surface.

5. CN concentrations in polluted and clean regions can be similar, demonstrating that CN counts alone do not reveal characteristics about the source, mass concentration, size, and other features of the aerosol.

6. The RCN/CN ratio is near 0.8 in the polluted region and about 0.1 in the clean region, demonstrating that RCN/CN provides a rapid and more unique signature for air mass and aerosol type than CN or RCN.

These observations characterize two major source regions for most nuclei that were not sea salt or Saharan dust. European continental pollution introduced a nuclei population related to combustion processes controlling the production of BC "seed" nuclei, while the clean mid-troposphere appeared to act as a source region for feeding surface layers with nuclei formed homogeneously aloft and possibly associated with extensive cloud outflow regions associated with cumulus convection [*Hegg et al.*, 1990, *Clarke*, 1993a, b; *Hudson*, 1993]. Modeling studies [*Raes and VanDingenen*, 1992; *Raes*, 1995] have also demonstrated the viability of this latter mechanism.

4. Discussion

4.1 Pollutant Nuclei and BC

Our ASTEX data also demonstrate that a refractory component was present as a constituent of most pollutant aerosol particles (Figures 1b and 3). Figure 11 shows a comparison of this refractory residual DMA mass with concurrent measurements of BC inferred from the aethaelometer data for a large number of horizontal flight legs made over a wide range of concentrations in the polluted air mass. If a density of about 2 g cm^{-3} is assumed for converting the refractory DMA volume to BC mass, then most inferred aethaelometer BC mass is within about a factor of 1 to 4 of the refractory DMA mass. This finding means that at times the refractory residual was virtually all light-absorbing black carbon, while at others it included other low light-absorbing refractory material. A relationship between BC and DMA refractory mass is reasonable for a combustion-derived pollution plume, since higher-temperature condensates (e.g., BC, soot, fly ash) will be the first to nucleate in a combustion plume and condense out

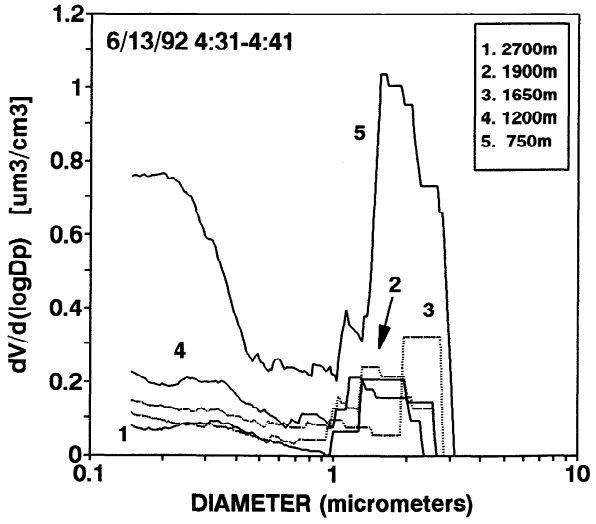

Figure 10. OPC volume distributions (μm^3 cm^{-3}) for data collected in descent for vertical profile (see text).

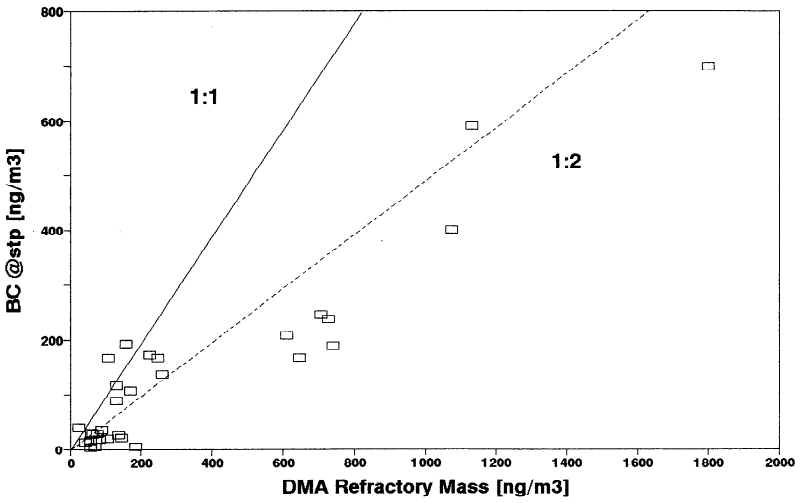

Figure 11. Aethaelometer BC versus DMA refractory mass for averages over horizontal legs.

during the initial cooling period. These newly formed particles (e.g., BC) are then available as condensation sites for lower temperature condensates (e.g., H_2SO_4) and a surface upon which further gas to particle conversion can proceed. Also, BC has been shown to be a catalyst for oxidation of SO_2 to sulfate [*Harrison and Pio*, 1983; *DeSantis and Allegrini*, 1992]. Hence the early generation of refractory nuclei by the combustion process could establish the majority of particles present in certain pollution plumes upon which the lower-temperature condensates can accumulate to make up the bulk of the resultant pollution aerosol mass.

As a result, combustion processes that produce large numbers of refractory nuclei for a given SO_2 (read as sulfate) source strength could ultimately result in a greater number of CN with a mass mean diameter smaller than that for combustion processes that produce fewer refractory primary nuclei. (Both the mass mean diameter and the number of available cloud condensation nuclei (CCN) are potentially significant aerosol properties that may have optical and climatological effects [*Penner et al.*, 1993]. Hence the relative production of RCN (as BC and fly ash) per mass of sulfate generated in different source regions may itself have an impact on assessment of sulfate emissions relevant to both radiative forcing of the formation of CCN and cloud albedo.

4.2 Other Observations

In dust layers here and over the Pacific [*Clarke*, 1993a] we found that greater mass loadings of coarse dust aerosol may often have relatively low CN. There are several possible reasons: (1) sourced from a region free of pollution and depleted in precursors for nucleation, (2) the large surface area of coarse dust aerosol can act as a sink for the smaller CN originally present in the air mass mixing with the dusts, (3) the dust may provide a reactive surface for heterogeneous reactions [*Dentener et al.*, 1996], thereby suppressing homogeneous nucleation. In any event, for these cases the RCN/CN ratio discussed earlier is often moderately high, but the CN concentration is relatively low [*Clarke*, 1993a]. These relationships between CN volatility and concentration can provide a simple indicator of air mass character both during real - time measurements on the aircraft and as a way of stratifying data in postflight analysis.

Several cases were described in which surface concentrations did not reflect the presence of higher concentrations aloft, often due to enhanced scavenging in the surface marine layer (e.g., Figure 8a). Variations in aerosol with altitude can be an important consideration in the interpretation of data collected at surface sites. For example, surface data from Tenerife (J. M. Prospero, personal communication, 1956) measured at an altitude of 2360 m indicate that many Saharan dust events are also associated with high sulfate and pollution aerosol. This observation would be expected for the dust case mentioned above [*Clarke et al.*, 1996a], which showed a mixed aerosol present at altitudes near 2000-2500 m. However, this mixture was representative only of aerosol at this altitude, apparently due to dust aerosol present aloft mixing into the pollution aerosol below. The dust layer at higher altitudes (Figure 4) was found to have very little sulfate, and the pollution below the transition layer had little dust (see Figure 8 of *Clarke et al.* [1996a]).

Variations in aerosol size and composition described above also embody a relationship between aerosol mass and the mass mean diameter. In Figure 12 we have averaged DMA mass distribution data for the ASTEX experiment into six mass intervals, each differing by about a factor of 2. A systematic increase in the mass mean diameter of the aerosol is evident for increasing total mass in the submicrometer sizes. This ASTEX data set is consistent with our general observation that cleanest air masses tend to have smaller mass mean diameters, while polluted air masses should tend to have larger mass mean diameters [*Porter and Clarke*, 1997]. Because certain important parameters describing aerosol optical effects (e.g., mass scattering coefficient [*Penner at al.*, 1993] depend upon mass mean diameter, this relationship could be included in models in which effective size distributions must be inferred from the more commonly available data on aerosol submicrometer mass.

5. Conclusions

We have presented data that describe key characteristics of the acrosol types present during the ASTEX/MAGE campaign and have described properties of interest to those measuring and modeling aerosol properties and fields over the North Atlantic. These include indications of the complex vertical and horizontal structure of the aerosol fields and the relationship to composition and size. Low concentrations in the marine surface layers and high concentrations aloft were documented as well as dust layers overlaying lower-level pollution layers. The complexity suggests that surface sites often fail to reflect column concentration or compositions and that comparisons of model column predictions and surface measurements must be interpreted with caution.

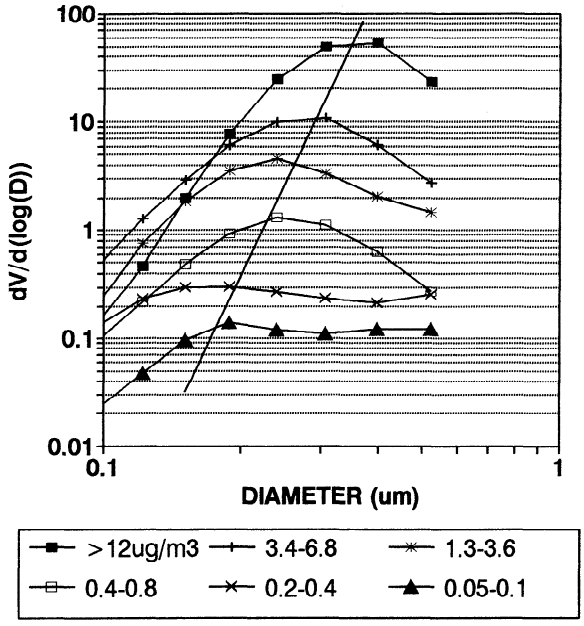

Figure 12. Dry volume distributions for all DMA data. These have been grouped, as indicated, into more commonly used mass intervals (based upon an assumed density of 1.8 g cm^{-1}). Higher mass concentrations are associated with increasing mass mean diameter.

Marked horizontal gradients were also evident and reflect features in aerosol fields that must be recognized in sampling strategies and predicted by the models.

High concentrations of small nuclei were encountered above the inversion in clean subsiding air from the central Atlantic. The gradient from aloft toward the inversion supports the notion that surface concentrations of CN removed by near-surface processes can be replenished by the entrainment of small nuclei formed aloft in clean regions [*Clarke*, 1993a, b; *Raes and VanDingenen*, 1992; *Raes*, 1995].

The high RCN/CN ratios observed were characteristic of air masses with surface-derived pollution or dust and lower ratios present in clean air characterized by homogeneously nucleated aerosol. This finding is consistent with previous measurements in the mid-troposphere over the Pacific and offers a simple way of identifying aerosol and air mass properties both in a real - time experimental mode and in postexperiment analysis. Clean marine regions were also characterized by low mass concentration of submicrometer aerosol tending to a sulfuric acid composition and with smaller particle diameters and few residual refractory particles.

The polluted European air mass had the highest submicrometer aerosol mass. This was dominated by a sulfate aerosol associated with a refractory component related to combustion-derived BC (soot). It appears possible that combustion processes may establish the refractory nuclei number concentration upon which most of the submicrometer mass (e.g., sulfate) in an aged plume will ultimately reside. If so, these particles (together with the condensed material) could establish the resulting mass mean diameter and thereby influence the number of CCN that may activate for a given supersaturation. This notion is consistent with the RCN/CN approaching 1 and moderately high CN and mass mean diameter that we observed in aged pollution. Mass mean diameter for all submicrometer aerosol was shown to generally increase with submicrometer mass in a predictable way that may provide a means for modeling size distributions based upon mass measurements (e.g., sulfate).

Appendix: Sampling Concerns for BC and CN

Earlier it was asserted that particle shatter was the source of elevated CN that we observed near clouds. Since new particle production has been argued to be present in the vicinity of clouds [*Hegg et al.*, 1990] and particle shatter has been also been argued to be the source of high concentrations observed near cloud by others [*Hudson*, 1993], we were concerned over the proper cause for our observations made on this experiment. The frequent presence of clouds in the marine boundary layer and the availability of both unheated CN and refractory RCN counters made possible to unambiguously identify the origin of high counts near cloud for this experiment.

As we noted in Figure 6, both CN and RCN were observed to increase in clouds. RCN are either soot, sea salt, or dust, and they do not nucleate in situ, so that rapid increases in RCN reflect either pockets of high aerosol concentrations or the result of some fragmentation process. Since mechanical disruption of dust or BC into many particles is unlikely, the reasonable candidate is a saline droplet. If it fragments, then numerous small saline droplets are produced and result in an increase of both CN and RCN upon evaporation. If this occurs, we would expect it to be more prevalent in marine regions of higher liquid water content (LWC) and associated larger drop sizes. Figure 13 is a plot of both CN and RCN as a function of LWC determined from the Electra FSSP for a period characterized by the spikes illustrated in Figures 7b, 8b, and 9. For low LWC there is no relationship evident but as LWC goes above 0.02 g/kg^{-1}, then both CN and RCN increase together. The RCN also becomes an increasing fraction of the total, confirming that droplet shatter is the cause. This behavior was observed not only in cloud but also below cloud in very light drizzle that was not visibly apparent but was evident in droplet probe data. For the NCAR Electra data during ASTEX, all of the cases we observed of sudden CN enhancement near cloud were attributable to the droplet-shattering mechanism. Other aircraft with different sample probes or flight speeds may or may not encounter the same problem.

A second measurement problem was observed in the aethaelometer (Magee Scientific) data. When changing altitudes,

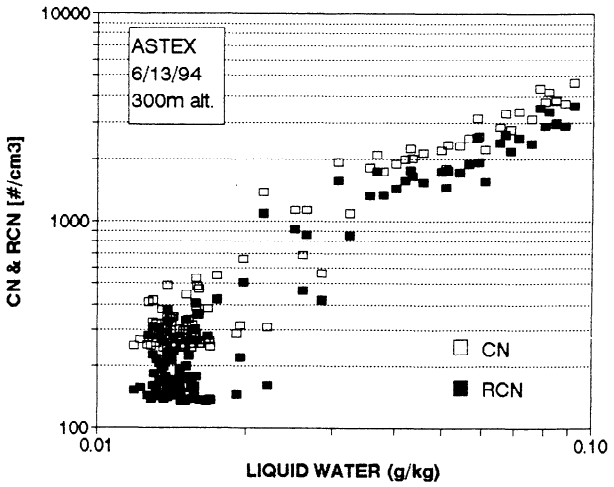

Figure 13. CN and RCN concentrations during period of droplet shatter and showing increases in both with liquid water content, as expected for shattering of saline droplet.

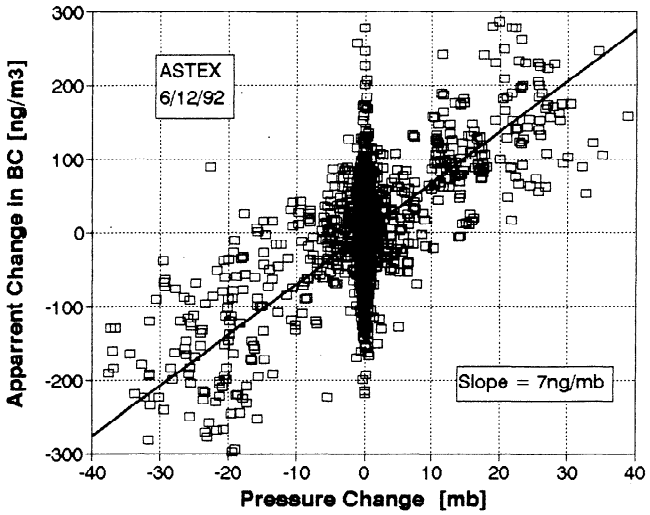

Figure 14. Apparent (spurious) change in BC caused by pressure (altitude) changes by aircraft.

we found that the BC concentrations observed during ascent were different from those during descent. A systematic behavior is evident if one plots the inferred BC versus the change in pressure (altitude) over some time interval for altitude changes in "clean air" having very low BC concentrations (Figure 14). Ideally, one would expect no dependency, but in fact a clear dependency exists. A comparison of different rates of climb/descent reveals that the slope of the relationship also appears to depend upon the rate of the altitude (pressure) change. First-order corrections are possible once a relationship is established, but the uncertainty for clear air data is large and contributes to the apparent BC variability in clear air shown in Figures 7a and 8b. Two possible causes are suggested. One is that small differential pressure changes over the aethaelometer filter may distort it and perturb the relative signal and sensor light intensities passing through the filter. The other is that the relative pressure changes between cabin and ambient pressure inside the detector head that holds the light source may result in flexing of the detector head and cause relative shifts in the detector intensities.

Another aethaelometer problem not illustrated here was discovered during the Lagrangian measurements that involved resampling of the same air mass. It was found that initial BC concentrations inferred from an initial pass through a layer with a new filter were invariably higher than the second pass with the same filter. This difference (up to 25%) persisted even after normalizing relative to changes in other aerosol measurements (e.g., CN). This discrepancy suggests that the light attenuation for a small amount of BC on a new filter is greater than that for the same amount of BC added later to the same filter. These were lightly loaded filters, and at no time did the final change in transmittance through the filter exceed 10%. While for many applications this will not be a significant problem, it makes the interpretation of small changes in BC obtained from aircraft during aerosol evolution difficult to quantify.

Acknowledgments. We are particularly grateful for the support of this work through funds provided through Ed Green and Gary Geernaert of the Office of Naval Research under contract ONR N00014-92-J-1388. Special appreciation is extended to Barry Huebert for facilitating our activities under ASTEX/MAGE and to the management of the National Center for Atmospheric Research Aviation Facility and the crew of the Electra for their cooperation in making these measurements possible. This research is a contribution to the International Global Atmospheric Chemistry Program (IGAC) Core project of the International Geosphere-Biosphere Programme (IGBP). SOEST Contribution No. 4524

References

Benkovitz, C.M., C.M. Berkowitcz, R.C. Easter, S. Nemesure, R. Wengener, and S.E. Schwartz, Sulfate over the North Atlantic and adjacent continental regions: evaluation for October and November, 1986 using a three-dimensional model driven by observation-derived meteorology, *J. Geophys. Res., 99*, 20,725-20,756, 1994.

Bergstrom, R.W., Extinction and absorption coefficients of the atmospheric aerosol as a function of size, *Contrib. Atmos. Phys., 46*, 223-234, 1973.

Bodhaine, B.A., Aerosol measurements at four background sites, *J. Geophys. Res., 88*, 10,753-10,768, 1983.

Bretherton, C.S., and R. Pincus, Cloudiness and marine boundary layer dynamics in the ASTEX Lagrangian experiments, 1, Synoptic setting and vertical structure, *J. Atmos. Sci., 52*, 2707-2723, 1995.

Chatfield, R.B. and P.J. Crutzen, Sulfur dioxide in remote oceanic air: Cloud transport of reactive precursors, *J. Geophys. Res., 89*, 7111-7132, 1984.

Clarke, A.D., A thermo-optic technique for in-situ analysis of size resolved aerosol physicochemistry, *Atmos. Environ. 25Part A*, 635-644, 1991.

Clarke, A.D., Atmospheric nuclei in the remote mid-troposphere, J. *Atmos. Chem., 14*, 479-488, 1992.

Clarke, A.D., Atmospheric nuclei in the Pacific mid-troposphere: Their nature, concentration, and evolution, *J. Geophys. Res., 98*, 20,633-20,647, 1993a.

Clarke, A.D., Equatorial convection as a source of nuclei over the remote Pacific, in *Proceedings of International Symposium on Dimethylsulfide, Oceans, Atmospheres and Climate: Belgirate, Italy, Oct. 1992*, Kluwer Acad., Norwell, Mass., 1993b.

Clarke, A.D., J.N. Porter, F. Valero, and P. Pillewski, Vertical profiles, aerosol microphysics, and optical closure during ASTEX: Measured and modeled column optical properties, *J. Geophys. Res., 101*, 4443-4453, 1996a.

Clarke, A.D., T. Uehara, and J.N. Porter, Lagrangian evolution of and aerosol column during ASTEX, *J. Geophys. Res., 101*, 4351-4362, 1996b.

d'Almeida, G.A., P. Koepke, and E.P. Shettle, *Atmospheric Aerosols Global Climatology and Radiative Characteristics*, A .Deepak, Hampton, Va., 1991.

Dentener, F.J., G.R. Charmichael, Y. Zhang, J. Lilieveld, and P. Crutzen, Role of mineral aerosol as a reactive surface in the global troposphere, *J. Geophys. Res., 101*, 22,869-22,899, 1996.

DeSantis, F., and I. Allegrini, Heterogeneous reactions of SO_2 and NO_2 on carbonaceous surfaces, *Atmos. Environ., Part A* 26, 3061-3064, 1992.

Harrison, R.M., and C.A. Pio, Kinetics of SO_2 oxidation over carbonaceous particles in the presence of H_2O, NO_2, NH_3, and O_3, *Atmos. Environ., Part A 27*, 1203-1212, 1993.

Hegg, D.A., L.F. Radke, and P.V. Hobbs, Particle production associated with marine clouds, *J. Geophys. Res., 95*, 13,917-13,926, 1990.

Hoppel, W.A., J.W. Fitzgerald, G.M. Frick, R.E. Larson, and E.J. Mack, Aerosol size distributions and optical properties found in the marine boundary layer over the Atlantic Ocean, *J. Geophys. Res., 95*, 3659-3686, 1990.

Hudson, J.G., Cloud condensation nuclei near marine cumulus, *J. Geophys. Res., 98*, 2693-2702, 1993.

Huebert, B.J., A. Pzenny and B. Blomquist, The ASTEX/MAGE Experiment,. *J. Geophys Res.,101*, 4319-4329, 1996.

Jensen, T.L., S.M. Kriedenweiss, Y. Kim, H. Sievering, and A. Pzenny, Aerosol distributions in the North Atlantic marine boundary layer during the Atlantic Statocumulus Transition Experiment/Marine Aerosol Gas Exchange, *J. Geophys. Res., 101*, 4455-4467, 1996.

Martin, G.M., D.W. Johnson, D.P. Rogers, P.R. Jonas, P.

Minnis, and D.A. Hegg, Observation of the interaction between cumulus clouds and warm stratocumulus clouds in the marine boundary layer during ASTEX, *J. Atmos. Sci., 52*, 2902-2922, 1994.

Penner, J.E., et al., Quantifying and minimizing uncertainty of climate forcing by anthropogenic aerosol, *DOE/NBB-0092T*, Nalt. Tech. Inf. Serv., Springfield, Va., 1993.

Porter, J.N. and A.D. Clarke, Aerosol size distribution models based on in - situ measurements, *J. Geophys. Res., 102*, 6035-6045, 1997.

Porter, J. N., A.D. Clarke, R. Pueschel, G. Ferry, and B.J. Huebert, Aircraft studies of size-dependent aerosol sampling through inlets, *J. Geophys Res., 97*, 3815-3824, 1992.

Prospero, J.M., and T.N. Carlson, Saharan air outbreaks over the tropical North Atlantic, *Pure Appl. Geophys., 119*, 677-691, 1981.

Raes, F., Entrainment of free tropospheric aerosols as a regulating mechanism for cloud condensation nuclei in the remote marine boundary layer, *J. Geophys. Res., 100*, 2893-2903, 1995.

Raes, F., and R. VanDingenen, Simulations of condensation and cloud condensation nuclei from biogenic SO_2 in the remote marine boundary layer, *J. Geophys. Res., 97*, 12,901-12,912, 1992.

Seinfeld, J.S., *Air Pollution*, pp. 281-286, John Wiley, New York, 1986.

Zhuang, L., and B.J. Huebert, Lagrangian analysis of the total ammonia budget during Atlantic Stratocumulus Transition Experiment/Marine Aerosol Gas Exchange, *J. Geophys. Res., 101*, 4341-4350, 1996.

A.D. Clarke, J.N. Porter, and T. Uehara, School of Ocean and Earth Science and Technology, University of Hawaii, 1000 Pope Road, Honolulu, HI 96822. (e-mail: tclarke@soest.hawaii.edu)

(Received February 13, 1997; revised May 19, 1997; accepted May 19, 1997.)